Published in final edited form as:
J Control Release. 2014 October 28; 192: 310–316. doi:10.1016/j.jconrel.2014.08.006.

Micro-fractional epidermal powder delivery for improved skin vaccination

Xinyuan Chen[a,1], **Garuna Kositratna**[b], **Chang Zhou**[a], **Dieter Manstein**[b], and **Mei X. Wu**[a,c,1]

[a]Wellman Center for Photomedicine, Massachusetts General Hospital, Department of Dermatology, Harvard Medical School, Boston, MA

[b]Cutaneous Biology Research Center, Department of Dermatology, Massachusetts General Hospital, Harvard Medical School, Boston, MA

[c]Harvard-MIT Division of Health Sciences and Technology, Cambridge, MA

Abstract

Skin vaccination has gained increasing attention in the last two decades due to its improved potency compared to intramuscular vaccination. Yet, the technical difficulty and frequent local reactions hamper its broad application in the clinic. In the current study, micro-fractional epidermal powder delivery (EPD) is developed to facilitate skin vaccination and minimize local adverse effects. EPD is based on ablative fractional laser or microneedle treatment of the skin to generate microchannel (MC) arrays in the epidermis followed by topical application of powder drug/vaccine-coated array patches to deliver drug/vaccine into the skin. The novel EPD delivered more than 80% sulforhodamine b (SRB) and model antigen ovalbumin (OVA) into murine, swine, and human skin within 1 hour. EPD of OVA induced anti-OVA antibody titer at a level comparable to intradermal (ID) injection and was much more efficient than tape stripping in both delivery efficiency and immune responses. Strikingly, the micro-fractional delivery significantly reduced local side effects of LPS/CpG adjuvant and BCG vaccine, leading to complete skin recovery. In contrast, ID injection induced severe local reactions that persisted for weeks. While reducing local reactogenicity, EPD of OVA/LPS/CpG and BCG vaccine generated a comparable humoral immune response to ID injection. EPD of vaccinia virus encoding OVA induced significantly higher and long-lasting interferon γ-secreting CD8+ T cells than ID injection. In conclusion, EPD represents a promising technology for needle-free, painless skin vaccination with reduced local reactogenicity and improved immunogenicity.

[1]Address Correspondence to: Xinyuan Chen, Wellman Center for Photomedicine, Massachusetts General Hospital, 55 Fruit Street, Thier 320, Boston, MA 02114, TEL: 617-726-5063; FAX: 617-726-1208; xchen14@partners.org; or Mei X. Wu, Wellman Center for Photomedicine, Massachusetts General Hospital, 50 Blossom Street, Edwards 222, Boston, MA 02114, TEL: 617-726-1298; FAX: 617-726-1208; mwu2@partners.org.

The authors have no conflict of interest to declare.

Keywords

skin vaccination; powder delivery; laser; microneedle; tape stripping; local reactogenicity; immunogenicity; vaccine adjuvant; drug delivery

Introduction

Vaccination plays a crucial role in global public health. Due to the convenience of injection, the majority of vaccines are delivered into the muscular tissue. Yet, it has long been recognized that vaccines delivered into the skin elicit more potent immune responses, at least partly attributed to the abundant antigen-presenting cells (APCs) within the skin [1–5]. Currently, three vaccines including Bacillus Calmette-Guérin (BCG) vaccine, rabies vaccine, and seasonal influenza vaccine, are approved for intradermal (ID) injection. Unfortunately, ID injection of these vaccines induced frequent local reactions. For instance, the live-attenuated mycobacterium *bovis* BCG vaccine induces severe local reactions that end with permanent scars in more than 90% vaccinees [6]. Rabies vaccine was recently approved for ID injection to spare vaccine doses and reduce costs because ID injection of one fifth dose of rabies vaccine induced a comparable anti-rabies antibody titer to full dose intramuscular (IM) vaccination [7]. Yet, ID rabies vaccination induces much higher rates of erythema, pruritus, and other local reactions than IM vaccination [7]. Very recently, a reduced dose of seasonal influenza vaccine (9μg instead of 15μg) was approved for ID injection by a newly developed ID microinjection system [8]. ID influenza vaccination induced an overall 30–75% erythema, induration, edema, and pruritus at local injection site, while IM injection induced <10% of these local reactions [8]. More frequent and severe local reactions following ID vaccination might breach the integrity of the skin and increase local infection risk. The unpleasant local reactions also reduce patient compliance, limiting the acceptance of the highly immunogenic route of vaccination in the clinic.

ID vaccination-associated local reactions also hamper the incorporation of adjuvants to further boost skin vaccination because the majority of adjuvants induce strong local reactions following ID injection (9–10). The most widely used aluminum salt-based Alum adjuvant, the recently approved AS04 adjuvant by adsorbing toll-like receptor 4 (TLR4) agonist monophosphoryl lipid A (MPL) onto Alum, and squalene-based oil-in-water emulsion adjuvant MF59 are not suitable for skin vaccination due to the long-term deposition and persisted local reactions at the injection site, as we have previously shown [9,10].

Novel skin delivery technologies capable of minimizing vaccine/adjuvant-induced local reactions while sustaining vaccine immunogenicity are highly demanded to explore the full potential of skin vaccination. In this study, we present a micro-fractional epidermal powder delivery, hereafter abbreviated as EPD, to meet the above needs. EPD is based on ablative fractional laser (AFL) or microneedle (MN) treatment of the skin to generate microchannel (MC) arrays in the epidermis followed by topical application of powder vaccine-coated array patches to deliver vaccines into the skin. Interstitial fluid is expected to be drawn into each MC after laser or MN treatment, where topically applied vaccine powders would be

dissolved and diffused from patches into MCs followed by entry into the surrounding tissue. Laser- and MN-generated MCs will be recovered in days because each MC is so small that it can be healed by surrounding normal skin [11–14]. This full repairing capacity forms the basis of cosmetic laser resurfacing and MN dermabrasion. Application of the micro-fractional repair concept to skin vaccination resulted in minimization of vaccine/adjuvant-induced local reactions without compromising vaccine immunogenicity and adjuvant potency. In this study, we found EPD could efficiently deliver a variety of molecules, like small molecular drug, various types of vaccines and adjuvants, into the skin and profoundly reduce local side effects of a combinatorial lipopolysaccharide (LPS) and CpG adjuvant (LPS/CpG) and BCG vaccine, while inducing comparable immune responses to ID injection.

Materials and methods

Animals and human skin samples

BALB/c mice (6–8 weeks old) were purchased from Charles River Laboratories. Yorkshire pigs (~4 months old) were obtained from Tufts. Animals were housed in animal facilities of Massachusetts General Hospital (MGH) and anesthetized for hair removal, laser treatment, and patch application. Freshly excised human skins from plastic surgery patients were obtained from Department of Dermatology of MGH. All animal procedures were approved by Institutional Animal Care and Use Committees of MGH and human skin study was approved by the Institutional Review Boards (IRBs) of MGH.

Reagents and laser device

Sulforhodamine B (SRB), OVA (Grade V), and LPS were purchased from Sigma (St. Louis, MO). Alexa Fluor 647-conjugated OVA (AF647-OVA) was obtained from Invitrogen (Carlsbad, CA). Murine-specific CpG 1826 and pig-specific CpG 2007 were obtained from Invivogen (San Diego, CA). BCG vaccine, which contains $1–8\times10^8$ colony forming units of BCG, was obtained from MGH Pharmacy. Vaccinia virus encoding OVA cDNA (VV-OVA) with a stock of $0.5–1\times10^9$ pfu/ml was a kind gift of Dr. Chance John Luckey (Brigham and Women's Hospital, Boston, MA). An UltraPulse Fractional CO_2 Laser (Lumenis Inc., Yorkneam, Israel) with laser energy at 5.0mJ and skin coverage at 5% was used to generate MC arrays in the skin surface. Sham laser treatment had the same procedure except the laser was not activated.

Powder array patch coating

Powder array patch coating was illustrated in figure 1. SRB was directly coated without prior treatment, while lyophilized OVA, LPS/CpG, OVA/LPS/CpG, VV-OVA were crushed into fine powders by pressing the lyophilized powders across the frosted ends of microscope slides. To prepare BCG vaccine patches, BCG vaccine was quickly taken from 4°C and fractionally coated without prior treatment and used instantly.

Topical patch application and ID injection

One 9×9 array patch was cut into four 4×4 array patches for topical delivery. The remaining 1×8 and 1×9 array patches were used to quantify the coating amount as shown below. To

evaluate the delivery efficiency, a 4×4 MC array in a 2×2 mm^2 area was generated followed by topical application of SRB- or OVA-coated 4×4 array patches onto laser- or sham-treated skin, or tape-stripped skin. The same tape stripping for 15 strokes (tape (1, 15)) and different tape stripping for 6 strokes by changing the tape every other stroke (tape (3, 6)) were used in the current study. To evaluate local reactogenicity, four 9×9 MC array in 2×2 cm^2 area were generated followed by topical application of four 8×8 LPS/CpG-coated array patches. Patch-coated OVA, LPS/CpG, and BCG vaccine were extracted into phosphate buffered saline (PBS) for ID injection to ensure the same vaccine and adjuvant doses were delivered in both groups.

Quantification of transcutaneous delivery

SRB delivered into the skin and remained on the patch were quantified following skin homogenization and patch extraction as previously described [13]. The delivery efficiency will be calculated as the relative SRB amount in the skin to that in skin plus patch. To calculate OVA delivery efficiency, OVA amount coated on the patch before delivery and remained on the patch after delivery was measured by a bicinchoninic acid (BCA) protein assay (Pierce). The difference between patch coated and patch remained reflected the delivered OVA amount, by which the delivery efficiency was calculated.

Immunogenicity and local reactogenicity

Antibody titers were measured by enzyme-linked immunosorbent assay (ELISA) by coating 100μg/ml OVA or 50μg/ml BCG vaccine. Cellular immune responses were evaluated by intracellular cytokine staining and flow cytometry. In brief, peripheral blood mononuclear cells (PBMCs) were isolated and stimulated overnight with OVA (100μg/ml) in the presence of 4μg/ml anti-CD28 antibody (37.51). Golgi-plug was added 5 hours before harvesting and cells were stained with PerCP/Cy5.5-anti-CD8 (53–6.7) and FITC-anti-IFNγ (XMG1.2) antibodies followed by flow cytometry analysis. Local reactions were monitored daily for at least 2 weeks. Pictures of local reactions were taken by a NIKON D5100 camera. In some studies, skins were dissected and subjected to standard histological analysis or real-time PCR analysis of pro-inflammatory cytokine expression as our previous report [15].

Vaccinia viral challenge

Mice were challenged 6 weeks after immunization on the same side with 10^6 pfu VV-OVA and skins were dissected 6 days after challenge. Viral load was quantified according to a published method [16]. In brief, total DNA was isolated and gene copy number specific to ribonucleotide reductase Vvl4L of VV (forward: 5'-GACACTCTGGCAGCCGAAAT-3'; reverse: 5'-CTGGCGGCTAGAATGGCATA-3') was quantified by SYBR Green real-time PCR analysis.

Quantification of inflammatory cell infiltration

Skin were dissected and subjected to paraffin sectioning and H&E staining as our previous report [15]. Total nucleated cells in 100×200$μm^2$ area in 5–7 randomly selected locations were quantified.

Scanning electron microscopy (SEM)

Laser-treated skin was fixed in Karnovsky's fixative followed by washing and dehydrating with ascending concentrations of alcohol. Samples were then critical-pointdried, coated with Chromium, and analyzed in a JEOL 7401F Field Emission Scanning Electron Microscope.

Statistical analysis

Values were expressed as Mean ± SEM (standard error of mean). Student t-test was used to analyze the difference between groups. P value was calculated by PRISM software (GraphPad, San Diego, CA) and considered significant if it was less than 0.05.

Results

Fractional patch coating

Pretreatment of the skin with safe technologies, like AFL and MN, to generate arrays of separated MCs in the skin surface has recently been explored to facilitate transcutaneous vaccine delivery [13,14,17–19]. Yet, the delivery efficiency remains a concern because vaccines are put on the entire surface [13,14,17–19]. To improve the delivery efficiency, we developed a simple coating strategy to coat powder vaccines in the same pattern as skin MCs. Here we use AFL-generated MCs as an example to illustrate the array patch fabrication process as shown in figure 1. A plastic membrane was exposed to laser to generate the same pattern of MC arrays as in the skin. The plastic membrane was then put atop of an adhesive patch and assembled. Vaccine powders were poured onto the assembly, laminated, followed by removal of non-adherent vaccine powders. The plastic membrane was then removed to obtain the powder vaccine array patches for topical application onto laser-treated skin. Such a coating doesn't need additives or excipients to form specific formulations. The coating procedure doesn't involve any harsh conditions either and can thus preserve vaccine immunogenicity and adjuvant potency. The simple coating can be readily expanded for large-scale manufacturing.

Efficient EPD of SRB

Model drug sulforhodamine b (SRB) was used to evaluate the efficiency of EPD first in laser-treated mouse, pig and human skin. An UltraPulse Fractional CO_2 laser was used to generate a 9×9 MC array in mouse skin (left, figure 2A) [13]. White-colored, small protrusions of the ruptured epidermis were clearly visible after laser treatment with tiny holes at the center of each protrusion (middle, figure 2A). Scanning electron microscope (SEM) imaging revealed oval-shaped MCs surrounded by elevated edges (right, figure 2A). The MC is about 31μm in diameter (average of both axes) and the protrusion is about 80–100μm in diameter when 2.5mJ laser energy was used. Increase of laser energy was found to enlarge both MC and protrusion. Powder SRB-coated array patches were made (figure 2B) and applied onto laser-treated skin. Black SRB powder became pink right after patch application due to quick dissolution by *in situ* tissue fluids. The pink color became darker and gradually expanded to the entire skin later on. Patches were removed 3 hours later and only trace amount of SRB remained on the patches applied onto laser-treated skin, while the same pattern of black SRB powder remained on patches applied onto sham-treated skin

(patch, figure 2C). In parallel, pink-colored SRB was found on the entire surface of laser-treated skin but not sham-treated skin with the strongest color inside laser-generated MCs (skin, figure 2C). Brightfield and fluorescence imaging of cross-sectioned pig and human skin at early (10 minutes) and late time points (3 hours) indicated that powder SRB was first delivered into laser-generated MCs and then dissipated to the surrounding tissue (supplemental figure 1). Skin delivery efficiency reached ~80% 1 hour after patch application, while <10% SRB deposited onto sham-treated skin within 6 hours (figure 2D). The efficiency and kinetics of EPD of SRB were comparable among mouse, pig, and human skin. EPD of SRB was further characterized in MN-treated skin. A row of 5 stainless steel MNs each with 750μm height, 200μm width, and 50μm thickness (figure 2E, kindly provided by Dr. Mark Prausnitz at Georgia Institute of Technology) was used to treat mouse and pig skin followed by topical application of 5 SRB-coated single row patches. As shown in figure 2F, most of the SRB (left side) disappeared from MN-generated MCs within 1 hour, concomitant with appearance of strong pink colored SRB around each MC in mouse and pig skin, despite some variation in individual SRB delivery at early time point (20min). In contrast, black SRB spots (right side) remained on the intact skin surface (figure 2F). We also explored two commercially available MN systems (3M™ Microchannel Skin System and 0.5mm Micro Needle Roller System) and we found these systems were less efficient than the stainless steel MN to facilitate topical powder SRB delivery (data not shown), possibly due to quick closure or insufficient fluid infusion into MN-generated MCs [11,12,20]. Yet, the above studies strongly indicated that powder SRB could be efficiently delivered into the skin via laser- and certain MN-generated MCs. To the best of our knowledge, such a quick and complete delivery of a hydrophilic drug following topical application hasn't been described before with any other technologies. In the following studies, we focused to explore EPD via laser-treated skin due to the consistent ablation of skin tissue without the risk of early closure of MCs.

Efficient EPD of OVA

We next evaluated EPD of model antigen OVA, a polypeptide with 385 amino acids and ~45 kDa molecular weight. After topical application of powder OVA-coated array patches, white-colored OVA quickly and completely disappeared from laser-generated MCs within 3 hours, while the same pattern of OVA remained on sham-treated skin (skin+patch, figure 3A). No OVA spots were found on patches applied onto laser-treated skin, but OVA spots remained with little change on patches applied onto sham-treated skin within the same period (patch, figure 3A). Such a delivery pattern was confirmed in pig and human skin. Quantification of the delivery efficiency indicated that more than 80% OVA was delivered into laser-treated skin within 1 hour regardless of the skin species, while less than 10% OVA was deposited onto sham-treated skin within 6 hours (figure 3B).

Besides AFL, tape stripping can also efficiently remove Stratum Corneum (SC) and facilitate transcutaneous vaccine delivery [21,22]. Thus, we compared AFL with tape stripping-based patch delivery in murine models. As shown in figure 3C, ~ half of the OVA spots disappeared from tape (3, 6)-treated skin and all OVA spots remained in the tape (1, 15)-treated skin within 30 minutes. Three hours after patch application, all OVA spots disappeared from tape (3, 6)-treated skin and only 2 OVA spots disappeared from tape (1,

15)-treated skin (figure 3C). Disappearance of OVA spots from tape (3, 6)-treated skin might reflect their exposure to more tissue fluids, as indicated in our previous report [13]. We further compared the spatial distribution of fluorescent AF647-OVA following AFL and tape (3, 6)-based delivery in MHC II-EGFP mice expressing MHC class II molecule infused into enhanced green fluorescent protein (a kindly gift of Drs. Boes and Ploegh), in which epidermal Langerhans cells (LCs) and dermal dendritic cells are clearly visible under a fluorescent microscope [15]. A localized vertical delivery was found in AFL group, while diffused horizontal delivery was observed in tape (3, 6) group (figure 3D). The diameter of AF647-OVA spots was much bigger in tape (3, 6) group than those in AFL group and a few spots were even connected to each other in tape (3, 6) group (left panel, figure 3D). AF647-OVA reached as deep as 81μm in AFL group, but only 27μm in tape (3, 6) group with the majority of OVA located on the skin surface without penetration into the skin (right panels, figure 3D). The localized vertical delivery in AFL exposed the majority of OVA to skin APCs, while the expanded horizontal distribution in tape (3, 6)-based delivery only exposed a small fraction of OVA to skin APCs. As a result, EPD induced a comparable anti-OVA antibody titer, while tape (1, 15) and (3, 6) induced 20 times lower anti-OVA antibody titer, as compared to ID injection of the same amount of OVA (figure 3E).

EPD reduces local side effects of adjuvants

We next explored whether micro-fractional delivery reduced local side effects of adjuvants. LPS/CpG (20μg/20μg) was fractionally coated onto the patches for EPD or extracted for ID injection. This dose was selected because ID injection of LPS/CpG induced erythema, swelling, and ulceration, which peaked on day 4 (figure 4A). On the contrary, the white-colored LPS/CpG adjuvant quickly disappeared through laser-generated MCs in EPD and induced only mild local reactions with no erythema, swelling, or ulceration (figure 4A). Skin in laser alone and EPD group fully recovered on day 12 and 21, respectively, while skin in ID group showed obvious morphology change on day 21 (figure 4A). Such a change in ID group might be permanent as there was no significant improvement on day 42. While reducing local side effects, EPD of OVA/LPS/CpG (10μg/20μg/20μg) induced a comparable anti-OVA antibody titer to ID injection of the same amount of OVA and LPS/CpG and much higher anti-OVA antibody titer than ID injection of OVA alone (figure 4B). We next evaluated whether EPD also reduced local reactions induced by a reduced dose of LPS/CpG (2μg/2μg). ID injection of LPS/CpG (2μg/2μg) induced skin color change but not swelling or ulceration. We found EPD significantly reduced inflammatory cytokine expression (e.g., CCL2, IFNγ, IL-1β, IL-6, TNFα) (figure 4C) and inflammatory cell infiltration (figure 4D). Quantification of nucleated cells in skin sections found that EPD reduced inflammatory cell infiltration by 3–4 times as compared to ID injection after subtracting the background level (35 vs. 10 cells per 0.02 mm^2, figure 4E).

Reduced local reactions following EPD of LPS/CpG were confirmed in pig skin by using pig specific CpG 7909. As in mouse skin, EPD of LPS/CpG (20μg/20μg) induced significantly reduced local reactions as compared to ID injection and comparable local reactions to laser treatment alone (figure 5A). Skin in EPD and laser alone group almost fully recovered on day 10. No abnormalities can be found in skin sections of the two groups on day 35 (figure 5B). In contrast, skin in ID group didn't fully recover on day 35 with

obvious infiltration of inflammatory cells and thickened epidermis (figure 5B). Due to the great similarity in epidermal and dermal thickness and APC density, composition, and function between pig and human skin [23,24], EPD is very likely to reduce adjuvant-induced local reactions in human skin.

EPD reduces local side effects while maintains immunogenicity of BCG vaccine

Significantly reduced local reactions following EPD of LPS/CpG prompted us to evaluate EPD of a clinical BCG vaccine that contains endogenous TLR2, 4, and 9 agonists and induces severe local reactions [25]. EPD of BCG vaccine induced minimal local reactions and skin fully recovered on day 11, while ID injection induced severe local reactions including erythema, swelling, and ulceration on day 5 and obvious skin morphology change on day 11 (figure 6A). While reducing local side effects, EPD induced a comparable anti-BCG antibody titer to ID injection of the same amount of BCG vaccine (figure 6B).

EPD increases cellular immune responses of VV-OVA immunization

After exploration of EPD of OVA and a live attenuated BCG vaccine, we analyzed EPD of a third type of vaccinia virus (VV)-based DNA vaccine. VV has been used as a viral vector to induce pathogen-specific cellular immunity and the delivery of VV through physically damaged epidermis (scarification) was found to induce the most potent immunity [16,26]. Due to the uncontrollable skin damage, scarification is not approved for use in modern world [10,16]. On contrary, AFL ablates superficial skin and generates photothermal damage in the epidermis that is highly controllable. For EPD of VV-OVA, VV-OVA was lyophilized in the presence of 10% trehalose to maintain viral activity [27]. EPD induced a slightly but significantly higher percentage of IFNγ-secreting CD8+ T cells than ID injection on day 5 (figure 7A).

The higher percentage of IFNγ-secreting CD8+ T cells was maintained for at least two weeks in EPD group, while quickly dropped to the baseline in ID group (figure 7A). After viral challenge, the viral load was 3.5×10^4 pfu/μg DNA in ID group and 9.6×10^3 pfu/μg DNA in EPD group, both of which are significantly lower than 4.8×10^5 pfu/μg DNA in control group (figure 7B). As compared to ID immunization, EPD reduced viral load by ~4 times (figure 7B).

Discussion

The current study introduces a novel skin delivery technology, called micro-fractional epidermal powder delivery or EPD, to improve safety of skin vaccination. The delivery uses laser- or MN-generated MCs in combination with powder vaccine array patches to deliver vaccines into the skin. AFL and MN pretreatment of the skin have been found to be safe and efficient for transcutaneous drug and vaccine delivery [13,14,17–19,28,29]. Yet, drugs and vaccines are applied on the entire skin surface in a liquid, cream, or lotion form with the majority (>90%) of drugs and vaccines undelivered because laser or MN only ablates <10% skin surface [13,14,17–19,28,29]. The fractional coating significantly increases the overall delivery efficiency and allows the majority of the drugs/vaccines to be delivered. EPD of SRB and OVA was found to reach >80% delivery efficiency in all skins tested including

human skin (figure 2D & 3B). Local tissue fluids are assumed to play a crucial role in EPD as suggested by the instant change of SRB from black to pink right after patch application. Beside SRB and OVA, EPD can efficiently deliver TLR agonists (e.g., LPS, IMIQ, and CpG), BCG vaccine, VV, poly(lactic-*co*-glycolic acid) nano- and micro-particles into the skin with little dependence on molecular weight, chemical structure, and particle size (data not shown).

By delivery of vaccines and adjuvants into separated MCs, EPD profoundly reduced local side effects of LPS/CpG adjuvant (figure 4A & 5) and BCG vaccine (figure 6A). Skin in EPD group fully recovered within 2–3 weeks, while skin in ID group was left with permanent scars (figure 4A, 5, & 6A), reminiscent of strong local reactogenicity of BCG vaccination in newborns[6]. Micro-fractional delivery might provide as a new concept to improve local safety of BCG vaccination. In the current study, BCG vaccine was delivered into laser-treated skin. Yet, we believe BCG vaccine delivered into MN-treated skin can also achieve similar delivery efficiency as in SRB delivery (figure 2F) and induce minimal local reactogenicity and full skin recovery, providing a cost-effective strategy for improved BCG vaccination in disease endemic areas. The mechanism of reduced local reactions and full skin recovery following EPD could be due to the following two reasons. First, EPD may induce a slow release of vaccines and adjuvants from laser-generated MCs as we found a significant amount of AF647-OVA remained inside MCs and slowly released for >7 days (supplemental figure 2). In contrast, ID injection instantly releases the entire vaccine/adjuvant and induces vigorous inflammation in the skin. Second, the micro-fractional delivery largely preserves skin repairing capacity by limiting vaccine/adjuvant-induced local reactions around each MC. In contrast, local reactions following ID injection occupy entire skin surface with an area of a few millimeter in diameter and it takes longer and is more difficult for new tissue to grow and replace the damaged skin.

EPD induces comparable immune responses to ID injection (figure 3E, 4B, 6B). The maintenance of vaccine immunogenicity while reducing local reactogenicity allows the incorporation of potent adjuvants to augment skin vaccination. In the current study, we found AFL was at least 20 times more efficient than tape stripping in enhancing transcutaneous OVA immunization due to sufficient OVA delivery into the skin in EPD. Although OVA powders were completely dissolved in tape-treated skin, the majority of OVA remained on the skin surface without penetration into the skin (figure 3F). The inability of OVA to penetrate into the skin is in line with recent findings that epidermal tissue also presents a significant barrier for transcutaneous macromolecule delivery after removal of SC layer [30]. Besides comparable immune responses induced by protein antigen and BCG vaccine, EPD of VV-OVA induced superior OVA-specific cellular immune responses and conferred better protection against viral challenges than ID injection. These studies strongly suggest great potentials for EPD in improvement of skin vaccination.

EPD has several advantages over liquid injections. Firstly, EPD is needle-free, painless because laser- or MN-generated MCs can be limited within epidermis, where no nerve ends exist, and powder vaccines can be dissolved *in situ* by interstitial fluids without causing skin wheals. In contrast, liquid vaccine injections induce pain and skin wheals [24,31]. Secondly, powder vaccines are more stable than liquid vaccines and might eliminate cold-chain storage

[32]. Even if cold-chain storage is required, powder vaccine patches can be sealed into a relatively small package to reduce cold-chain volumes [32–34]. Elimination of cold-chain storage or reduction of cold-chain volumes is expected to greatly reduce shipping and storage costs, enabling cost-effective immunization in resource-poor developing countries, especially when EPD is combined with MN treatment. Thirdly, direct powder vaccine delivery eliminates programmatic errors during reconstitution and injection due to the use of wrong diluents for reconstitution and wrong syringes for injection (different from the one used for reconstitution) [35]. EPD also has unique features as compared to dissolving MNs, in which various additives, like tackifiers and plasticizers, are fabricated with vaccines to form sharp needles to penetrate the skin [36]. Incorporation of additives reduces the encapsulated vaccine amount and potentially increases MN number and skin area involved to deliver required vaccine doses [37]. In contrast, powder array patch coating for EPD eliminates additives, excipients, or specific formulations and involves no complex manufacturing. Such a coating can be conveniently expanded for large-scale Good Manufacturing Practice (GMP) production.

EPD is potentially suitable to deliver any vaccines considering the fact that many current vaccines are already manufactured, shipped, and stored in a lyophilized powder form and various technologies are available to transform liquid vaccines into a dry form, like freeze-drying, spray-drying, and spray-freeze-drying [32–34,38]. Laser ablation and patch application can be integrated into a handheld device that costs only a few hundred dollars for clinical use. Considering the device can be used for hundreds of thousands of times, each immunization cost will be only minimal. Powder array patch delivery can also be integrated with skin-piercing MNs, which might provide a more simple and cost-effective strategy for clinical translation of this technology. EPD is promising for safer and more effective skin vaccination.

Conclusion

The current study evaluates the delivery efficiency, local reactogenicity, and immunogenicity of a novel micro-fractional epidermal powder delivery or EPD in skin vaccination. More than 80% drug and vaccine doses can be delivered into the skin by this method. Due to the micro-fractional delivery, EPD profoundly reduces local side effects of vaccines and adjuvants and induces complete skin recovery. In contrast, ID injection induces severe local reactions, leaving permanent scars. Importantly, EPD well-maintains vaccine immunogenicity and adjuvant potency by inducing an at least comparable immune response to ID injection. These features warrant further investigation of EPD to improve skin vaccination considering skin vaccination often induces frequent and severe local reactions.

Supplementary Material

Refer to Web version on PubMed Central for supplementary material.

Acknowledgments

We thank Photopathology Core in our Department for tissue sectioning and flow cytometry services. This work is supported in part by the National Institutes of Health grants AI070785, AI089779, and RC1 DA028378 (to M.X.W), and Bullock-Wellman Fellowship, National Institutes of Health grants DA033371, AI107678 (to X.Y.C.).

Reference List

1. Kim YC, Prausnitz MR. Enabling skin vaccination using new delivery technologies. Drug Deliv. Transl. Res. 2011; 1:7–12. [PubMed: 21799951]
2. Chen D, Maa YF, Haynes JR. Needle-free epidermal powder immunization. Expert. Rev. Vaccines. 2002; 1:265–276. [PubMed: 12901567]
3. Glenn GM, Rao M, Matyas GR, Alving CR. Skin immunization made possible by cholera toxin. Nature. 1998; 391:851. [PubMed: 9495336]
4. Karande P, Mitragotri S. Transcutaneous immunization: an overview of advantages, disease targets, vaccines, and delivery technologies. Annu. Rev. Chem. Biomol. Eng. 2010; 1:175–201. [PubMed: 22432578]
5. Kendall MA. Needle-free vaccine injection. Handb. Exp. Pharmacol. 2010:193–219. [PubMed: 20217531]
6. Jeena PM, Chhagan MK, Topley J, Coovadia HM. Safety of the intradermal Copenhagen 1331 BCG vaccine in neonates in Durban, South Africa. Bull. World Health Organ. 2001; 79:337–343. [PubMed: 11357213]
7. Lang J, Hoa DQ, Gioi NV, Vien NC, Nguyen CV, Rouyrre N, Forrat R. Immunogenicity and safety of low-dose intradermal rabies vaccination given during an Expanded Programme on immunization session in Viet Nam: results of a comparative randomized trial. Trans. R. Soc. Trop. Med. Hyg. 1999; 93:208–213. [PubMed: 10450451]
8. Leroux-Roels I, Vets E, Freese R, Seiberling M, Weber F, Salamand C, Leroux-Roels G. Seasonal influenza vaccine delivered by intradermal microinjection: A randomised controlled safety and immunogenicity trial in adults. Vaccine. 2008; 26:6614–6619. [PubMed: 18930093]
9. Chen X, Wu MX. Laser vaccine adjuvant for cutaneous immunization. Expert. Rev. Vaccines. 2011; 10:1397–1403. [PubMed: 21988305]
10. Chen X, Wang J, Shah D, Wu MX. An update on the use of laser technology in skin vaccination. Expert. Rev. Vaccines. 2013; 12:1313–1323. [PubMed: 24127871]
11. Gupta J, Gill HS, Andrews SN, Prausnitz MR. Kinetics of skin resealing after insertion of microneedles in human subjects. J. Control Release. 2011; 154:148–155. [PubMed: 21640148]
12. Kalluri H, Banga AK. Formation and closure of microchannels in skin following microporation. Pharm. Res. 2011; 28:82–94. [PubMed: 20354766]
13. Chen X, Shah D, Kositratna G, Manstein D, Anderson RR, Wu MX. Facilitation of transcutaneous drug delivery and vaccine immunization by a safe laser technology. J. Control Release. 2012; 159:43–51. [PubMed: 22261281]
14. Kim YC, Park JH, Prausnitz MR. Microneedles for drug and vaccine delivery. Adv. Drug Deliv. Rev. 2012; 64:1547–1568. [PubMed: 22575858]
15. Chen X, Kim P, Farinelli B, Doukas A, Yun SH, Gelfand JA, Anderson RR, Wu MX. A novel laser vaccine adjuvant increases the motility of antigen presenting cells. PLoS. One. 2010; 5:e13776. [PubMed: 21048884]
16. Liu L, Zhong Q, Tian T, Dubin K, Athale SK, Kupper TS. Epidermal injury and infection during poxvirus immunization is crucial for the generation of highly protective T cell-mediated immunity. Nat. Med. 2010; 16:224–227. [PubMed: 20081864]
17. Lee WR, Shen SC, Pai MH, Yang HH, Yuan CY, Fang JY. Fractional laser as a tool to enhance the skin permeation of 5-aminolevulinic acid with minimal skin disruption: a comparison with conventional erbium:YAG laser. J. Control Release. 2010; 145:124–133. [PubMed: 20359510]
18. Hessenberger M, Weiss R, Weinberger EE, Boehler C, Thalhamer J, Scheiblhofer S. Transcutaneous delivery of CpG-adjuvanted allergen via laser-generated micropores. Vaccine. 2013; 31:3427–3434. [PubMed: 23273971]

19. Ding Z, Verbaan FJ, Bivas-Benita M, Bungener L, Huckriede A, van den Berg DJ, Kersten G, Bouwstra JA. Microneedle arrays for the transcutaneous immunization of diphtheria and influenza in BALB/c mice. J. Control Release. 2009; 136:71–78. [PubMed: 19331846]
20. Martanto W, Moore JS, Couse T, Prausnitz MR. Mechanism of fluid infusion during microneedle insertion and retraction. J. Control Release. 2006; 112:357–361. [PubMed: 16626836]
21. Behrens RH, Cramer JP, Jelinek T, Shaw H, von Sonnenburg F, Wilbraham D, Weinke T, Bell DJ, Asturias E, Pauwells HL, Maxwell R, Paredes-Paredes M, Glenn GM, Dewasthaly S, Stablein DM, Jiang ZD, Dupont HL. Efficacy and safety of a patch vaccine containing heat-labile toxin from Escherichia coli against travellers' diarrhoea: a phase 3, randomised, double-blind, placebo-controlled field trial in travellers from Europe to Mexico and Guatemala. Lancet Infect. Dis. 2013
22. Frerichs DM, Ellingsworth LR, Frech SA, Flyer DC, Villar CP, Yu J, Glenn GM. Controlled, single-step, stratum corneum disruption as a pretreatment for immunization via a patch. Vaccine. 2008; 26:2782–2787. [PubMed: 18455283]
23. Marquet F, Bonneau M, Pascale F, Urien C, Kang C, Schwartz-Cornil I, Bertho N. Characterization of dendritic cells subpopulations in skin and afferent lymph in the swine model. PLoS. One. 2011; 6:e16320. [PubMed: 21298011]
24. Laurent PE, Bonnet S, Alchas P, Regolini P, Mikszta JA, Pettis R, Harvey NG. Evaluation of the clinical performance of a new intradermal vaccine administration technique and associated delivery system. Vaccine. 2007; 25:8833–8842. [PubMed: 18023942]
25. Trinchieri G, Sher A. Cooperation of Toll-like receptor signals in innate immune defence. Nat. Rev. Immunol. 2007; 7:179–190. [PubMed: 17318230]
26. Draper SJ, Heeney JL. Viruses as vaccine vectors for infectious diseases and cancer. Nat. Rev. Microbiol. 2010; 8:62–73. [PubMed: 19966816]
27. Pearson FE, McNeilly CL, Crichton ML, Primiero CA, Yukiko SR, Fernando GJ, Chen X, Gilbert SC, Hill AV, Kendall MA. Dry-coated live viral vector vaccines delivered by nanopatch microprojections retain long-term thermostability and induce transgene-specific T cell responses in mice. PLoS. One. 2013; 8:e67888. [PubMed: 23874462]
28. Haedersdal M, Sakamoto FH, Farinelli WA, Doukas AG, Tam J, Anderson RR. Fractional CO(2) laser-assisted drug delivery. Lasers Surg. Med. 2010; 42:113–122. [PubMed: 20166154]
29. Lee WR, Pan TL, Wang PW, Zhuo RZ, Huang CM, Fang JY. Erbium:YAG laser enhances transdermal peptide delivery and skin vaccination. J. Control Release. 2008; 128:200–208. [PubMed: 18471920]
30. Andrews SN, Jeong E, Prausnitz MR. Transdermal delivery of molecules is limited by full epidermis, not just stratum corneum. Pharm. Res. 2013; 30:1099–1109. [PubMed: 23196771]
31. Kis EE, Winter G, Myschik J. Devices for intradermal vaccination. Vaccine. 2012; 30:523–538. [PubMed: 22100637]
32. McAdams D, Chen D, Kristensen D. Spray drying and vaccine stabilization. Expert. Rev. Vaccines. 2012; 11:1211–1219. [PubMed: 23176654]
33. Alcock R, Cottingham MG, Rollier CS, Furze J, De Costa SD, Hanlon M, Spencer AJ, Honeycutt JD, Wyllie DH, Gilbert SC, Bregu M, Hill AV. Long-term thermostabilization of live poxviral and adenoviral vaccine vectors at supraphysiological temperatures in carbohydrate glass. Sci. Transl. Med. 2010; 2:19ra12.
34. Sou T, Meeusen EN, de Veer M, Morton DA, Kaminskas LM, McIntosh MP. New developments in dry powder pulmonary vaccine delivery. Trends Biotechnol. 2011; 29:191–198. [PubMed: 21255854]
35. Craig L, Elliman D, Heathcock R, Turbitt D, Walsh B, Crowcroft N. Pragmatic management of programmatic vaccination errors--lessons learnt from incidents in London. Vaccine. 2010; 29:65–69. [PubMed: 21040692]
36. Sullivan SP, Koutsonanos DG, Del Pilar MM, Lee JW, Zarnitsyn V, Choi SO, Murthy N, Compans RW, Skountzou I, Prausnitz MR. Dissolving polymer microneedle patches for influenza vaccination. Nat. Med. 2010; 16:915–920. [PubMed: 20639891]
37. Hickling JK, Jones KR, Friede M, Zehrung D, Chen D, Kristensen D. Intradermal delivery of vaccines: potential benefits and current challenges. Bull. World Health Organ. 2011; 89:221–226. [PubMed: 21379418]

38. Chen D, Kristensen D. Opportunities and challenges of developing thermostable vaccines. Expert. Rev. Vaccines. 2009; 8:547–557. [PubMed: 19397412]

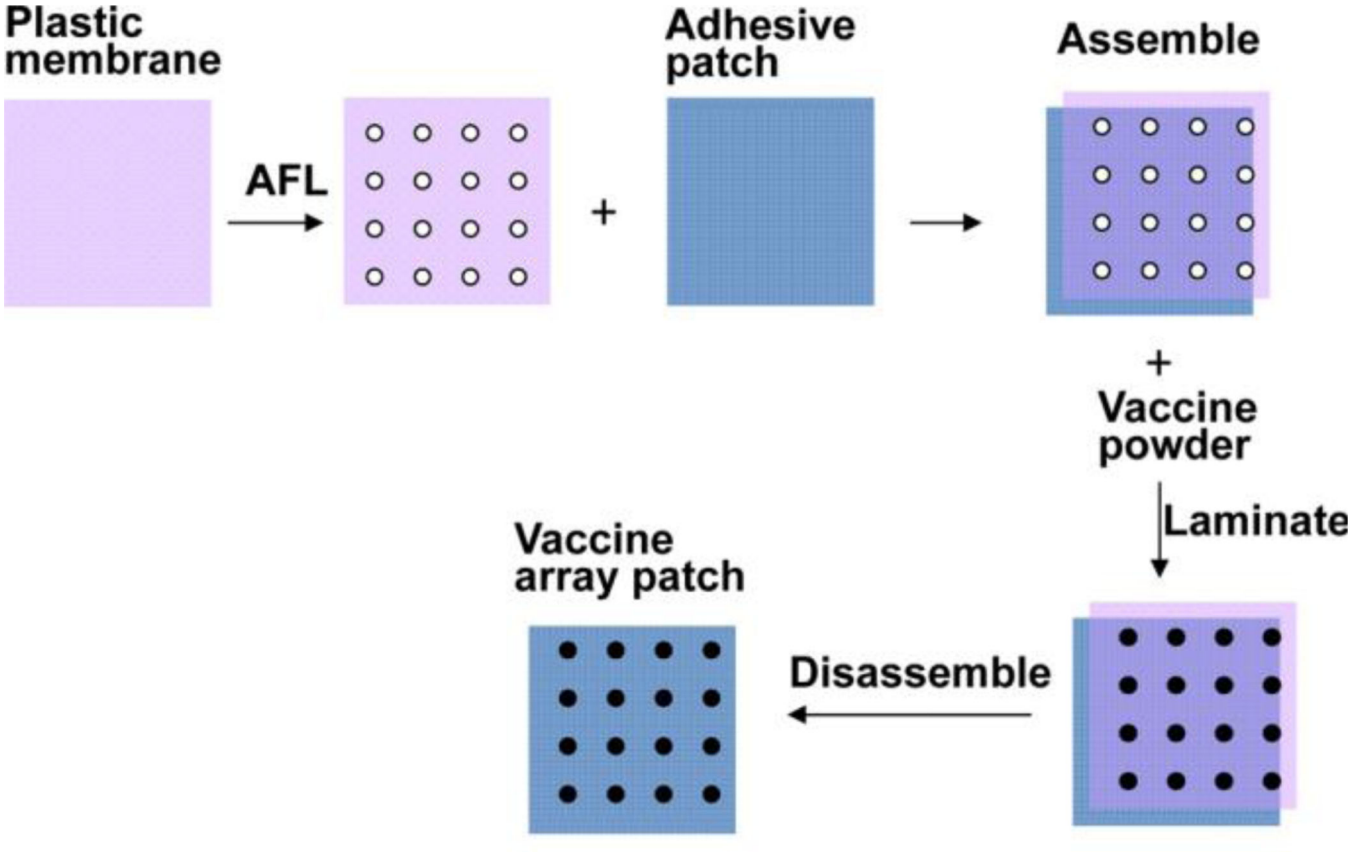

Figure 1. Illustration of powder array patch coating

A plastic membrane was exposed to laser illumination (35mJ, 5%) to generate 4×4 array of microholes in ~2×2 mm^2 area, each with a measured diameter of 189μm. The membrane was topically layered onto an adhesive patch (3M). Vaccine powders were poured onto the membrane/patch assembly and pushed to fill the microholes. Non-adherent powders were removed before disassembly of the plastic membrane/adhesive patch assembly to obtain powder vaccine coated array patches.

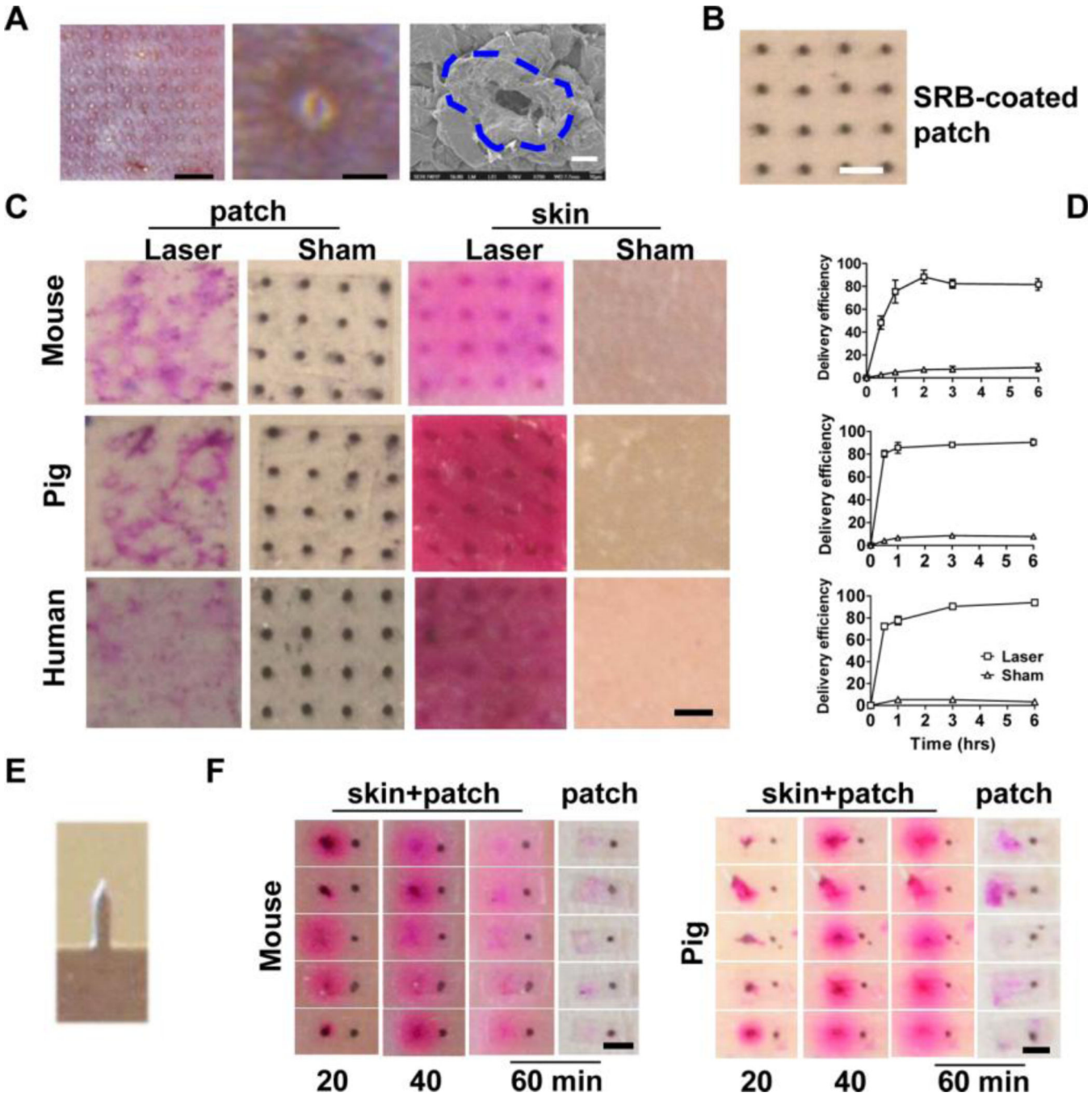

Figure 2. EPD of SRB

A. Characteristics of laser-generated MCs in mouse skin. Left, laser generated a 9×9 MC array (scale: 1.5mm); Middle, enlarged protrusion with a tiny microhole at the center (scale: 125μm); Right, representative SEM image of a MC with elevated edges outlined by dashed line (scale: 20μm). **B**. Representative powder SRB-coated array patch. Scale: 750μm. **C**. SRB-coated patches were topically applied onto laser- or sham-treated mouse, pig, and human skin. Three hours later, patches were removed and representative patch and skin pictures were shown. Scale: 750μm. **D**. At indicated times, SRB-coated patches were

removed and the delivery efficiency was calculated after quantification of SRB amount in the skin and on the patch. n=4. **E**. Image of one MN in a row of 5. **F**. A row of 5 MNs as in **E**. was used to pierce live mouse skin and dissected pig skin followed by topical application of 5 single row patches each with 2 SRB coating spots. One spot (on the left) was put just above MN-generated MC and the other (on the right) was put on intact skin surface. Images were taken 20, 40, and 60 minutes later. Patches were further removed and patch pictures were taken. Scale: 750μm.

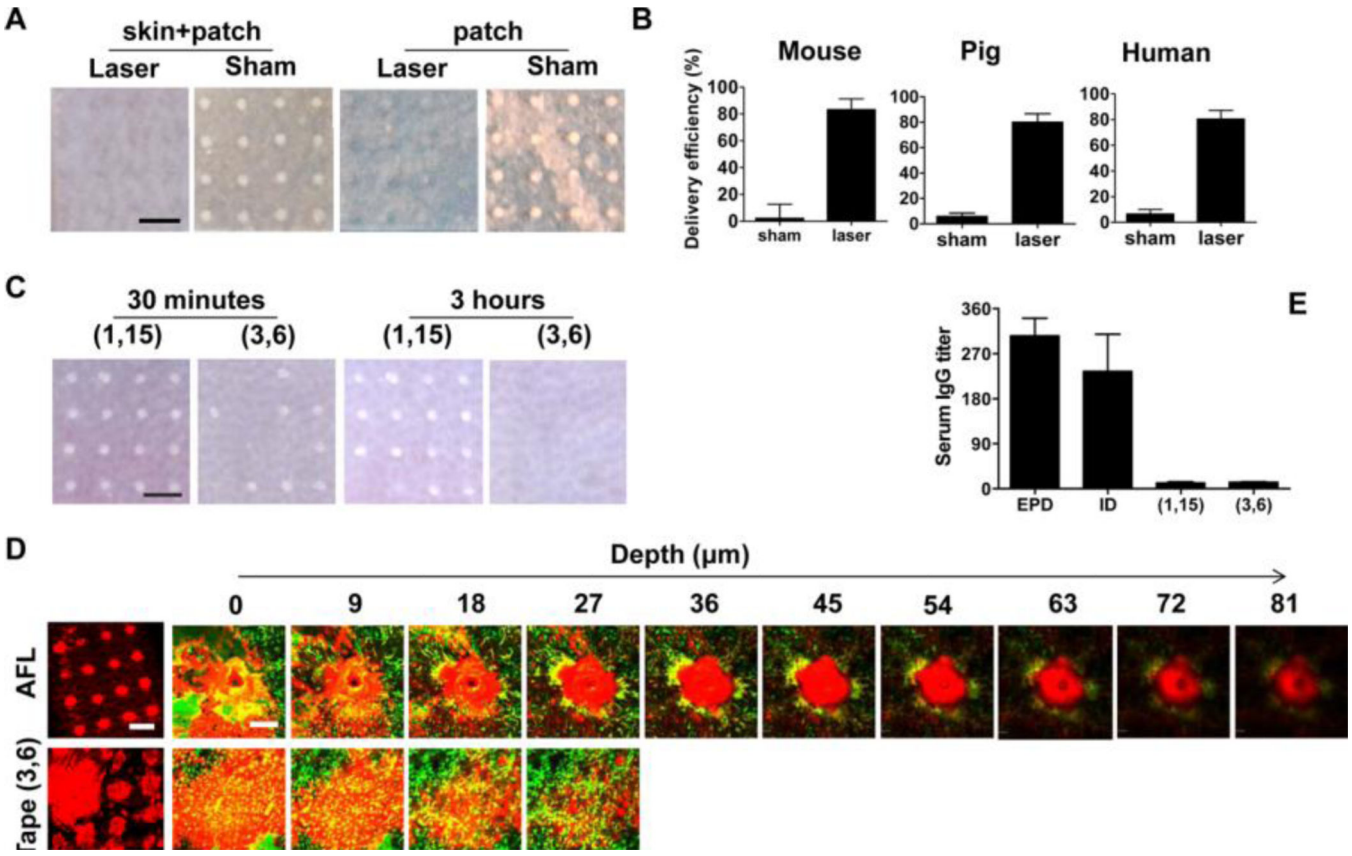

Figure 3. EPD of OVA

A. Powder OVA-coated array patches were topically applied onto laser- or sham-treated skin. Three hours later, skin pictures with patch attached (skin+patch) and patch pictures (patch) after patch removal were shown. Scale: 750μm. **B**. OVA patches were removed 1 hour after application and the amount of OVA remained on the patches was measured to calculate the delivery efficiency. **C**. Skin was subjected to tape stripping followed by topical application of the same OVA array patches as in A. Thirty minutes and 3 hours later, skin pictures were taken. **D**. Powder AF647-OVA-coated array patches were topically applied onto laser-treated or tape (3, 6)-treated skin of MHC II-EGFP mice for 6 hours. Skin pictures were taken at superficial level (left panel, scale: 750μm) or at different depths (right panels, scale: 100μm) under intravital confocal microscope. Green: GFP-labeled APCs; red: AF647-OVA. **E**. Mice were immunized with EPD or tape stripping-based powder delivery of OVA or intradermally injected with the same amount of OVA. Two weeks later, serum anti-OVA IgG titer was measured. n=5.

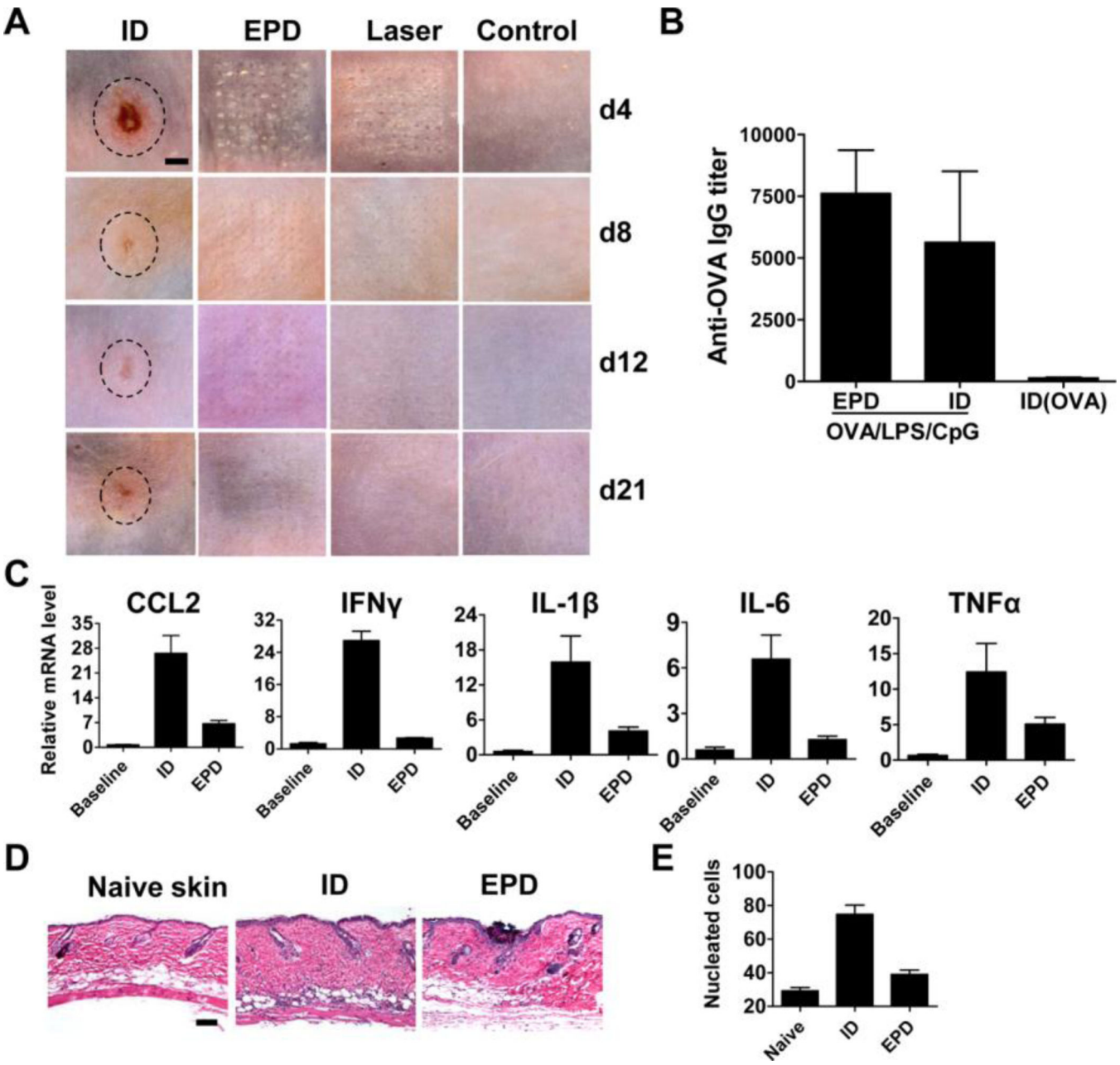

Figure 4. EPD reduces local reactogenicity of LPS/CpG adjuvant in mice

A. Mice were treated with laser followed by topical application of LPS/CpG (20μg each)-coated array patches (EPD), or intradermally injected with patch extracts (ID), or treated with laser alone, or left untreated. Skin pictures were taken on day 4, 8, 12 and 21 and representative local reactions were shown. The edges of the local reactions in ID group were outlined by dashed lines. Scale: 1.5mm. **B**. Mice were treated with laser followed by topical application of OVA/LPS/CpG (10μg/20μg/20μg)-coated array patches (EPD) or intradermally injected with patch extracts (ID), or intradermally injected with the same amount of OVA (ID(OVA)). Two weeks later, serum anti-OVA IgG titer was measured. n=4. **C**. Mice were treated with laser followed by topical application of LPS/CpG-coated

array patches (2μg each), or intradermally injected with the same amount of LPS/CpG mixture, or left untreated. 24 hours later, skin was dissected and expression of CCL2, IFNγ, IL-1β, IL-6 and TNFα was quantified. n=2–4. **D**. Mice were similarly treated as in **C**. 24 hours later, skin was dissected and subjected to histological analysis. Representative H&E-stained sections were shown. Scale: 100μm. **E**. Total nucleated cells in sections from **D.** were calculated. n=5–7.

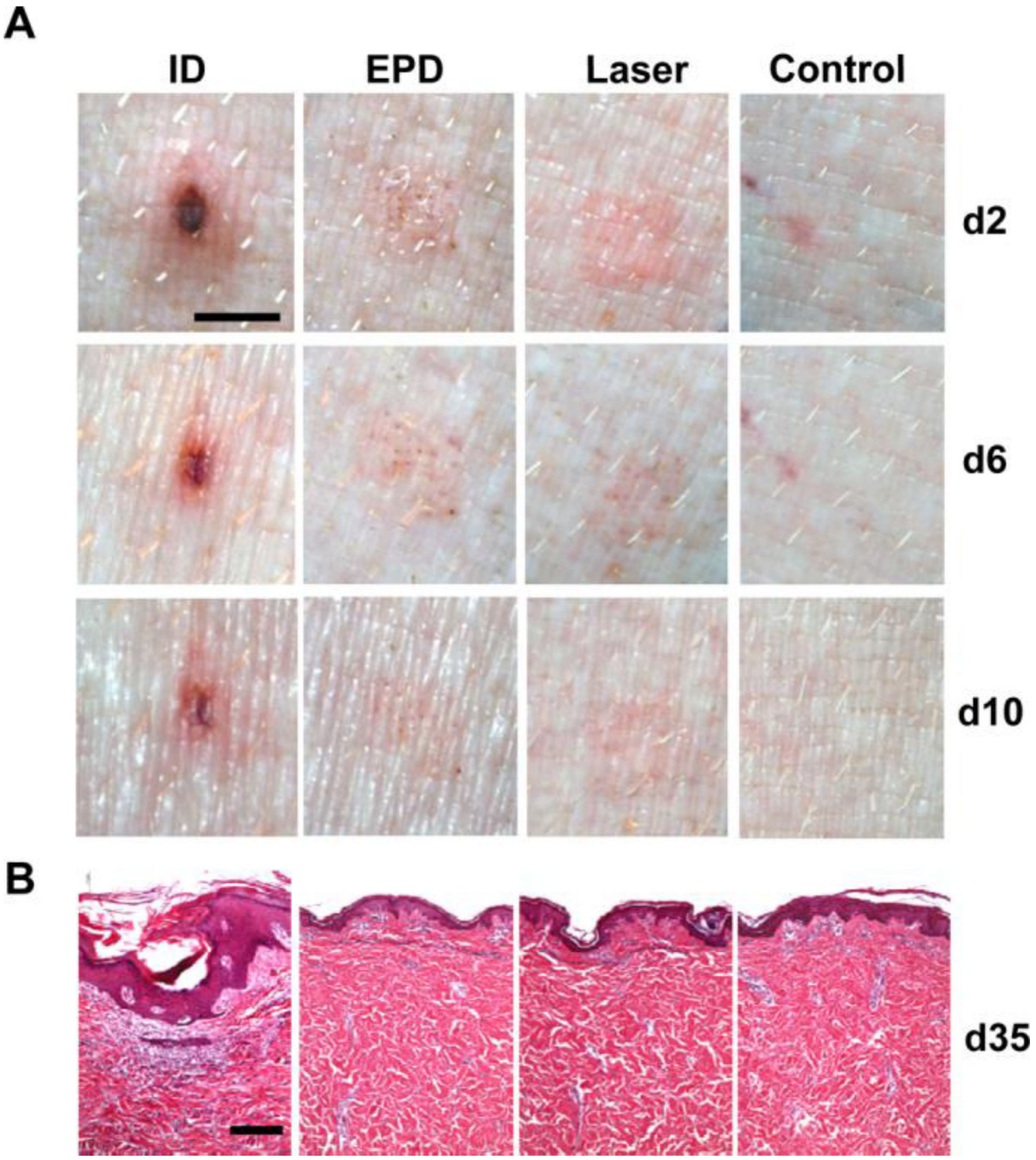

Figure 5. EPD reduces local reactogenicity of LPS/CpG adjuvant in pigs

Pigs were treated with laser followed by topical application of LPS/CpG(20μg each)-coated array patches, or intradermally injected with LPS/CpG from patch extracts, or treated with laser alone, or intradermally injected with PBS. **A**. Representative local reactions on day 2, 6, and 10 were shown. Scale: 3mm. **B**. pigs were sacrificed on day 35 and skin samples were collected and subjected to histological analysis. Representative skin H&E sections were shown. Scale: 200μm.

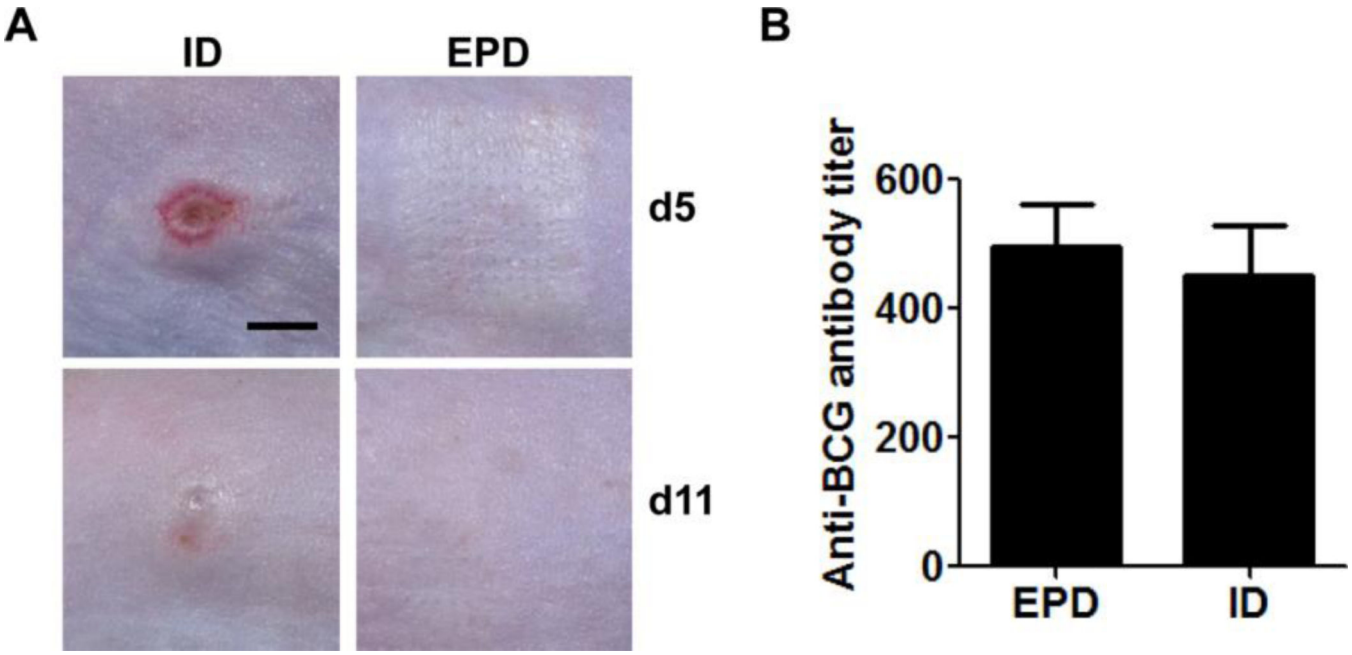

Figure 6. EPD reduces local side effects of BCG vaccine in mice

Mice were treated with laser followed by topical application of BCG vaccine-coated array patches or intradermally injected with BCG vaccine from patch extracts. Skin reactions were monitored daily and representative local reactions on day 5 and 11 are shown in **A** (scale: 3mm). Serum anti-BCG antibody titer was measured 2 weeks after immunization and shown in **B**. n=4

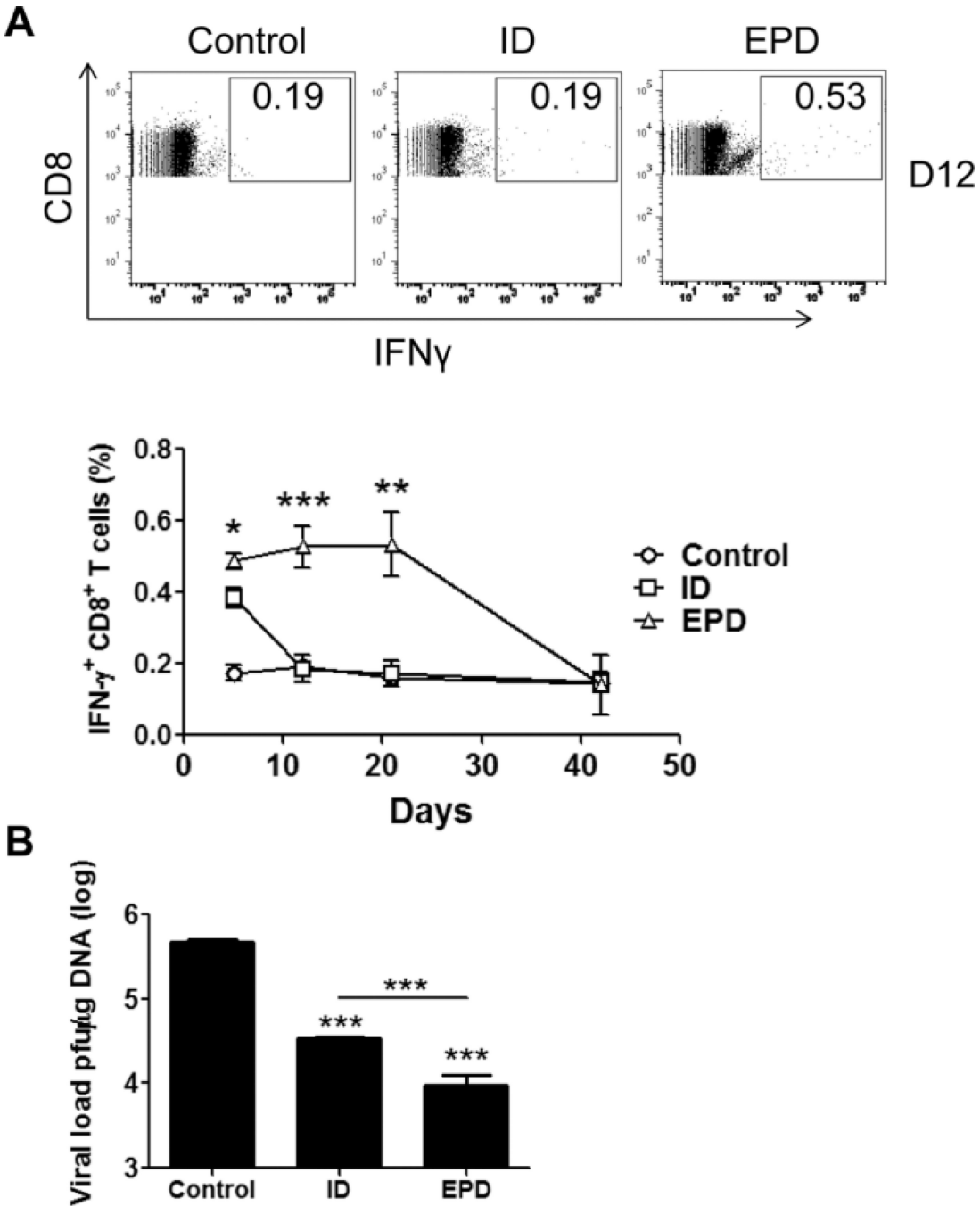

Figure 7. EPD improves immunogenicity of VV-OVA in mice

A. Mice were immunized with EPD of VV-OVA or intradermally injected with the same amount of VV-OVA. 5, 12, 21 days later, percentage of IFNγ-secreting CD8+ T cells in PBMCs was analyzed by flow cytometry. Representative flow cytometry figures (upper) and the percentage of IFNγ-secreting CD8+ T cells (lower) were shown. **B**. Mice were challenged 6 week after immunization and viral load 6 days after challenge was shown. n=4.